IEEE Access
Multidisciplinary | Rapid Review | Open Access Journal

Received October 12, 2020, accepted October 29, 2020, date of publication November 18, 2020,
date of current version December 15, 2020.

Digital Object Identifier 10.1109/ACCESS.2020.3038925

Control of the Vehicle Inertial Suspension Based on the Mixed Skyhook and Power-Driven-Damper Strategy

XIAOFENG YANG[1], HANG SONG[1], YUJIE SHEN[2], YANLING LIU[1], AND TAO HE[1]
[1]School of Automotive and Traffic Engineering, Jiangsu University, Zhenjiang 212013, China
[2]Automotive Engineering Research Institute, Jiangsu University, Zhenjiang 212013, China

Corresponding author: Yanling Liu (liuyl@ujs.edu.cn)

This work was supported in part by the National Natural Science Foundation of China under Grant 51705209, Grant 52072157, and Grant 52002156, in part by the China Postdoctoral Science Foundation under Grant 2019M651723 and Grant 2020M671355, in part by the Jiangsu Postdoctoral Science Foundation under Grant 2020Z246, and in part by the Zhenjiang Key Research and Development Program under Grant GY2019006.

ABSTRACT With the development of the traditional semi-active suspensions, different kinds of control algorithms have been proposed and applied, including skyhook (SH), acceleration-driven-damper (ADD), power-driven-damper (PDD), the mixed SH and ADD (SH-ADD), mixed SH and PDD (SH-PDD), and others. Among them, the vibration suppression in a wide frequency domain is realized by the SH-ADD or the SH-PDD, but the latter is more effective. Subsequently, the vehicle inertial suspension has been found to have better vibration suppression performance than the conventional suspension in the low frequency band. In order to suppress body vibration in a wide frequency domain to improve overall ride comfort, the inertial suspension using SH-PDD is proposed to further improve the vibration isolation performance due to its superiority of low frequency resistance in this article. First, an inertial suspension model of SH-PDD strategy is established, and the superior characteristics of an inertial suspension in a low frequency range are verified in numerical analysis. Then, the impact of the damping coefficient of the SH-PDD control strategy on the dynamic output performance of an inertial suspension is studied. In addition, the parameters of the proposed inertial suspension are optimized by means of the particle swarm optimization (PSO) method. By designing the error dynamic equation and sliding mode switching function, a sliding mode variable structure controller for an inertial suspension is finally constructed. Simulation results show that compared with the SH-PDD conventional suspension and the conventional suspension, the RMS value of body acceleration of the SH-PDD inertial suspension is reduced by 16.6% and 32.2% respectively, and the reduction is mainly in a low frequency range. Therefore, the proposed inertial suspension possesses better attenuation ability for the vehicle body vibrations to improve ride comfort.

INDEX TERMS Inertial suspension, SH-PDD, particle swarm optimization, sliding mode control.

I. INTRODUCTION

Since 1973, first proposed by Karnopp and Crosby, the semi-active vehicle suspension has been widely studied to improve ride comfort. Its idea is to adjust the damping or stiffness according to different road conditions to obtain an optimal vibration isolation performance [1]. In order to further improve the vehicle ride comfort, many different control algorithms have been proposed to effectively suppress body vibrations. Firstly, the skyhook (SH) control has great vibration isolating benefits around the resonance of the sprung mass due to its damping force opposite to the sprung mass velocity is generated to reduce the acceleration of the sprung mass [2], [3]. Unlike the SH control, the acceleration-driven-damper (ADD) control suppressed the resonance and amplitude in the middle and high frequency bands [4]. Subsequently, combining the advantages of SH and ADD, the mixed SH and ADD (SH-ADD) control strategy was proposed in [5], which preliminary realized the performance of the traditional suspension to suppress the sprung mass acceleration across the whole frequency spectrum. However, Morselli pointed out that the ADD strategy causes body chattering, which deteriorates ride comfort, and proposed a power-driven-damper (PDD) strategy [6].

The associate editor coordinating the review of this manuscript and approving it for publication was Jianyong Yao.

Correspondingly, Liu applied the idea of the SH-ADD to the PDD, and proposed the mixed SH and PDD control strategy to eliminate chattering and suppress body vibration in a wide frequency band [7]. In addition, robust control and Model Predictive Control (MPC) are widely used in vehicle control. Peng and Chen designed the corresponding controller to obtain better handling stability [8], [9].

Although, in recent years, many control algorithms have been developed, but the performance improvement space of the semi-active conventional suspension has reached a bottleneck, which is caused by the ''spring-damping'' parallel inherent structure. To this end, domestic and foreign scholars have conducted a great deal of research, but have not broken through the limitations of the traditional suspension form. Until 2002, Professor Smith of Cambridge University invented a two-terminal mass element ''inerter'' [10], breaking the original ''spring-damping'' parallel inherent form. This article refers to the suspension with the inerter as an inertial suspension. Due to the low frequency resistance of the inerter, the inertial suspension can better suppress vibration to improve ride comfort compared with traditional suspension at the vehicle body bias frequency.

After more than 10 years of development, the structure of an inerter has gradually diversified, including rack-and-pinion inerters [11], ball-screw inerters [12], and hydraulic inerters [13]. In [14]–[17], the suspension employing an inerter element performs better than a traditional passive suspension. More recently, mechatronic inerters [18] and hydraulic electric inerters [19], [20] were invented respectively, laying a foundation for the controllable inertial vehicle suspension system. Since then, an inertial suspension of the SH control with the aim of suppressing the vibration of the vehicle body is developed by Hu *et al.* [21]. In [22], a semi-active inertial suspension using a hybrid control strategy was built, effectively improving the overall performance of the vehicle. Li of the Hong Kong University proposed a semi-active inertial suspension with adaptive inertance for improving ride comfort [23]. The ADD strategy was applied to the inertial suspension, and the vibration suppression in the wide frequency domain of the inertial suspension was initially achieved, but an ADD inertia suspension will cause chattering just like the traditional suspension, which worsens the ride comfort [24].

In general, SH-PDD strategy can perfectly suppress the vehicle body vibration in the traditional suspension, but the inertial suspension only has the effect of suppressing vibration at the low frequency band. To isolate a wider frequency vibration of the inertial suspension system, the SH-PDD strategy is combined with an inertial suspension, and the active control mechanism of the controllable inertial suspension is constructed to suppress the amplitude of the vehicle body acceleration in a wide frequency bands to further improve the vehicle ride comfort.

This article is organized as follows. First, an ideal suspension model and SH-PDD strategy is proposed in Section II. Then, the impact of the control strategy damping coefficient on the dynamic output performance of the inertial suspension is studied in Section III. Moreover, the parameters of the proposed inertial suspension are optimized in Section IV. In addition, a sliding mode variable structure control mechanism is adopted to realize the coordinated control of the inertial suspension, and the performance of the inertial suspension is simulated and analyzed in section V. Finally, main conclusions are drawn in Section VI.

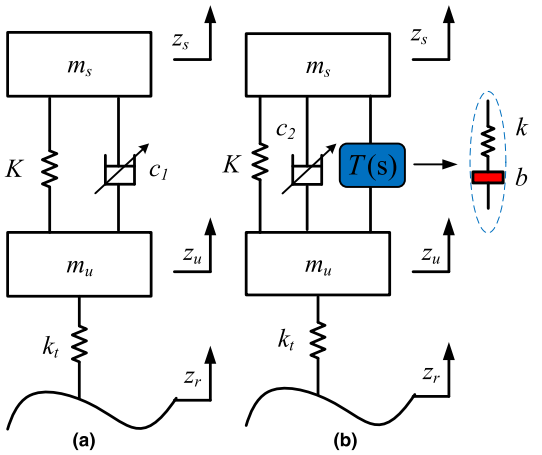

FIGURE 1. Quarter suspension models. (a)the conventional suspension. (b) the interial suspension.

II. SUSPENSION MODEL AND SH-PDD STRATEGY STATEMENT

A. SYSTEM MODEL

Quarter models of a conventional suspension and an inertial suspension, depicted in Fig. 1, are utilized to the ideal model in this article. The dynamic motion is respectively governed by the following equations:

$$\begin{cases} m_s\ddot{z}_s + K(z_s - z_u) + c_1(\dot{z}_s - \dot{z}_u) = 0 \\ m_u\ddot{z}_u + K(z_u - z_s) + k_t(z_u - z_r) \\ \qquad +c_1(\dot{z}_u - \dot{z}_s) = 0 \end{cases} \tag{1}$$

$$\begin{cases} m_s\ddot{z}_s + K(z_s - z_u) + Y(s)(\dot{z}_s - \dot{z}_u) \\ \qquad +c_2(\dot{z}_s - \dot{z}_u) = 0 \\ m_u\ddot{z}_u + k_t(z_u - z_r) - K(z_s - z_u) \\ -Y(s)(\dot{z}_s - \dot{z}_u) - c_2(\dot{z}_s - \dot{z}_u) = 0 \end{cases} \tag{2}$$

where m_s is the sprung mass, m_u is the unsprung mass, K is the spring stiffness of the suspension, k_t is the spring stiffness of the tire, c_1 and c_2 are the controllable damping coefficient; z_s and z_u represent the vertical displacements of the body and the tire, respectively. z_r is the uneven road displacement. $Y(s)$ in equation (2) denotes the velocity-type impedance of the series structure of the inerter (b) and the auxiliary spring(k) [25].

B. SH-PDD STRATEGY

Before deriving the SH-PDD control law of an inertial suspension, it is necessary to analyze the abilities of a vehicle suspensions from the perspective of the energy dissipation between the sprung mass and the unsprung mass.

Therefore, according to the power equation, the power of each component in the suspension system is analyzed [7]. As shown in Fig. 1, the sprung mass vibration power absorbed by the suspension spring is:

$$P_{ss} = K(z_s - z_u)\dot{z}_s \tag{3}$$

The sprung mass vibration power absorbed by the suspension semi-active damper is:

$$P_{sd} = c_i(\dot{z}_s - \dot{z}_u)\dot{z}_s, (i = 1, 2) \tag{4}$$

The sprung mass vibration power absorbed by the inertial suspension speed-type impedance is:

$$P_{st} = T(s)(\dot{z}_s - \dot{z}_u)\dot{z}_s \tag{5}$$

The vibration power released by the suspension spring to the unsprung mass is:

$$P_{us} = K(z_s - z_u)\dot{z}_u \tag{6}$$

The vibration power released by the semi-active suspension damper to the unsprung mass is:

$$P_{ud} = c_i(\dot{z}_s - \dot{z}_u)\dot{z}_u, \quad (i = 1, 2) \tag{7}$$

The vibration power released by the inertial suspension speed-type impedance to the unsprung mass is:

$$P_{ut} = T(s)(\dot{z}_s - \dot{z}_u)\dot{z}_u \tag{8}$$

Therefore, the net power of the conventional suspension is:

$$\begin{aligned} P_{net1} &= P_{ss} + P_{sd} - P_{us} - P_{ud} \\ &= K\,(z_s - z_u)\,(\dot{z}_s - \dot{z}_u) + c_1(\dot{z}_s - \dot{z}_u)^2 \end{aligned} \tag{9}$$

The net power of the inertial suspension is:

$$\begin{aligned} P_{net} &= P_{ss} + P_{sd} + P_{st} - P_{us} - P_{ud} - P_{ut} \\ &= K(z_s - z_u)(\dot{z}_s - \dot{z}_u) + c_2(\dot{z}_s - \dot{z}_u)^2 \\ &\quad + T(s)(\dot{z}_s - \dot{z}_u)^2 \end{aligned} \tag{10}$$

From the perspective of energy dissipation, the vehicle suspension has the ability to decouple the energy between the sprung mass and the unsprung mass, which is represented by P_{net}. The closer the value of P_{net} is to zero, the better the energy isolation of the vehicle suspension. Therefore, the power suspension damping control law for the SH-PDD traditional suspension is shown as:

$$c_1 = \begin{cases} c_{\max}, \textit{ if } \dot{z}_s^2 - \dot{z}_u^2 \geq 0 \text{ or } K(z_s - z_u)(\dot{z}_s - \dot{z}_u) \\ \qquad + c_{\max}(\dot{z}_s - \dot{z}_u)^2 < 0 \\ c_{\min}, \textit{ if } \dot{z}_s^2 - \dot{z}_u^2 < 0 \text{ and } K(z_s - z_u)(\dot{z}_s - \dot{z}_u) \\ \qquad + c_{\min}(\dot{z}_s - \dot{z}_u)^2 \geq 0 \\ \dfrac{-K(z_s - z_u)}{(\dot{z}_s - \dot{z}_u)}, \text{otherwise} \end{cases} \tag{11}$$

Similarly, the SH-PDD control law for an inertial suspension is explicitly given by:

$$c_2 = \begin{cases} c_{\max}, \textit{ if } \dot{z}_s^2 - \dot{z}_u^2 \geq 0 \text{ or } K(z_s - z_u)(\dot{z}_s - \dot{z}_u) \\ \qquad + c_{\max}(\dot{z}_s - \dot{z}_u)^2 + T(s)(\dot{z}_s - \dot{z}_u)^2 < 0 \\ c_{\min}, \textit{ if } \dot{z}_s^2 - \dot{z}_u^2 < 0 \text{ and } K(z_s - z_u)(\dot{z}_s - \dot{z}_u) \\ \qquad + c_{\min}(\dot{z}_s - \dot{z}_u)^2 + T(s)(\dot{z}_s - \dot{z}_u)^2 \geq 0 \\ \dfrac{-K(z_s - z_u) - T(s)(\dot{z}_s - \dot{z}_u)}{(\dot{z}_s - \dot{z}_u)}, \text{otherwise} \end{cases} \tag{12}$$

TABLE 1. Simulation parameters.

Parameter	Value
Sprung mass m_s[kg]	320
Unsprung mass m_u[kg]	45
Suspension spring stiffness K [N/m]	22000
Equivalent tire stiffness k_t [N/m]	190000
Inertance b [kg]	91
Maximum damping coefficient c_{max} [N·s/m]	4000
Minimum damping coefficient c_{min} [N·s/m]	300
Suspension auxiliary spring stiffness k [N/m]	165

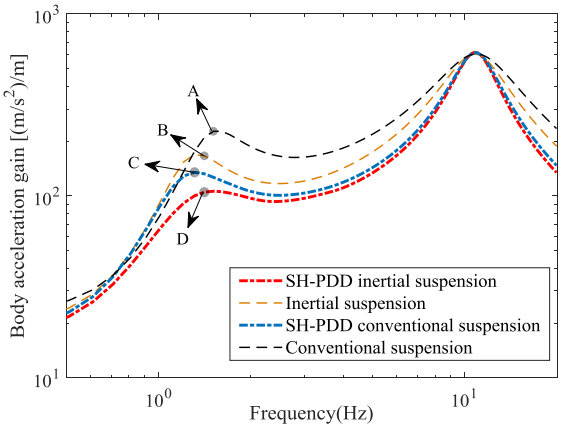

FIGURE 2. Acceleration gain of the SH-PDD control suspension and the passive suspension.

TABLE 2. Performance comparison at low frequency formant (near 1Hz).

	Value [(m/s²)/m]	Improvement
A (Conventional suspension)	226.3	/
B (Inertial suspension)	175.5	22.4%
C (SH-PDD conventional suspension)	134.7	40.5%
D (SH-PDD inertial suspension)	104.7	53.7%

According to the above control law, the SH-PDD traditional suspension and the SH-PDD inertial suspension were simulated respectively. The parameters of the proposed suspension are cited from [7], [16], as listed in Table 1. The results are plotted in Fig. 2.

As can be seen from Fig. 2, compared to the passive suspension, the SH-PDD conventional suspension not only reduces the body acceleration amplitude near the natural frequency of the sprung mass (1Hz), but also improves the body acceleration at high frequency bands. However, in Table 2, the resonance peak of the inertial suspension at a low frequency is reduced by 22.4%, proving that an inertial suspension can effectively suppress resonance at a low frequency range. Moreover, the SH-PDD inertial suspension further

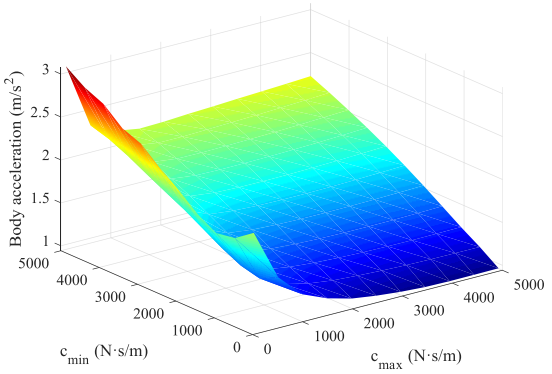

FIGURE 3. The Change of RMS of body acceleration based on SH-PDD Strategy.

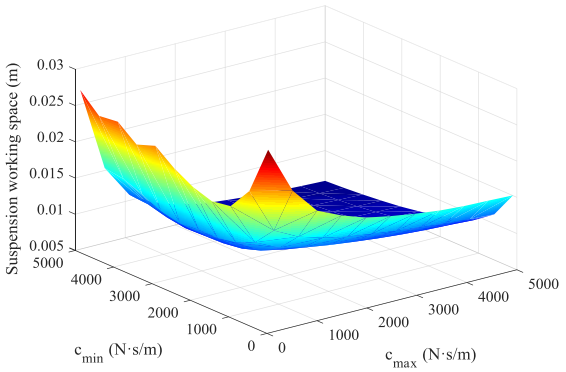

FIGURE 4. The Change of RMS of suspension working space based on SH-PDD Strategy.

reduces the peak value by 53.7% at the body resonance frequency and further improves the ride comfort.

In brief, an inertial suspension using the SH-PDD strategy further suppresses the body acceleration at a low frequency band, and the performance in the medium and high frequency bands is also better than a traditional SH-PDD suspension.

III. ANALYSIS OF THE INFLUENCR OF DAMPING PARAMETERS ON THE DYNAMIC PERFORMANCE

In order to further investigate the performance of the proposed inertial suspension with SH-PDD strategy, the $c_{\max}$ and $c_{\min}$ of the damping coefficient in the control strategy are taken as 100 to 5000 N·s/m respectively, and the impact of damping coefficient on the vibration response characteristics of an inertial suspension is analyzed. The simulation results are shown in in Fig. 3 to Fig. 5.

As demonstrated in Fig. 3 to Fig. 5, the RMS value of body acceleration of an inertial suspension based on SH-PDD strategy decreases with the increase of $c_{\max}$ and increases with the increase of $c_{\min}$; However, for the suspension working space, the RMS value continuously decreases with the increase of $c_{\min}$; the RMS value of dynamic tire load decreases first and then remains unchanged with the increase of $c_{\max}$ and $c_{\min}$. In general, when both $c_{\max}$ and $c_{\min}$ are small, the RMS value of body acceleration, suspension working space and dynamic tire load are not low; With the $c_{\min}$ increased, the suspension working space and dynamic tire load are improved, but the

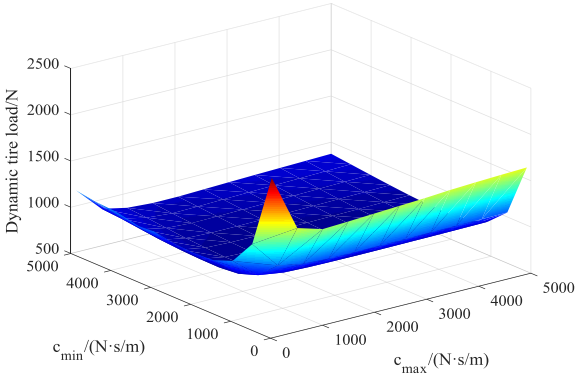

FIGURE 5. The Change of RMS of dynamic tire load e based on SH-PDD Strategy.

vehicle body acceleration are deteriorated, so on the premise of satisfying the requirements of the vehicle suspension working space and dynamic tire load, the value of $c_{\min}$ should be minimized as much as possible to reduce the RMS value of the body acceleration.

IV. PARAMETER OPTIMIZATION OF INERTIAL SUSPENSION MODEL

In addition to the value of the damping coefficient, the performance of an inertial suspension based on the SH-PDD control strategy is also related to the value of other relevant parameters. In order to achieve the optimal performance of the proposed inertial suspension model, the parameters of the suspension need to be optimized. In this article, the particle swarm optimization (PSO) algorithm suitable for dynamic and multi-objective environments is utilized to optimize the structural parameters of a vehicle suspension system [26]–[28]. Particle Swarm Optimization is a swarm intelligence optimization algorithm. Its basic idea is to select particles randomly in a given solution space to initialize, and update its position attribute by tracking the individual extremum and global extremum. After several iterations, the optimal particle is finally found. The particle velocity and position are updated in accordance with the following two formulas:

$$V^{n+1} = \lambda V^n + d_1 r_1 (P_{id}^n - X^n) + d_2 r_2 (P_{gd}^n - X^n) \quad (13)$$

$$X^{n+1} = X^n + V^{n+1} \quad (14)$$

where λ is the inertia factor, V is the velocity of the particle, d_1 and d_2 are the learning factor or the acceleration constant, r_1 and r_2 represent the random number between (0,1), n represents the number of iterations, P_{id} and P_{gd} are the individual extremum and global extremum. X is the current position of the particle.

In order to convert the multi-objective function into a single-objective function, the inertance (b), the maximum value of damping coefficient ($c_{\max}$), the minimum value of damping coefficient ($c_{\min}$), the stiffness of suspension spring(K) and the stiffness of auxiliary spring(k) in the inertial suspension are taken as the individual to be solved, and the RMS value of body acceleration is taken as optimization

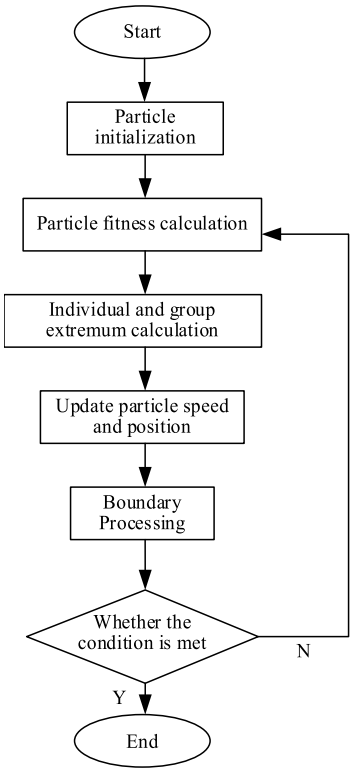

FIGURE 6. Parameter optimization flow chart.

objectives to improve the vehicle ride comfort. The ratio of performance index before optimization and after optimization is utilized to the fitness function of the PSO algorithm, and its expression and constraint conditions are as follows:

$$\min J = \frac{BA(P)}{BA_{pass}} \tag{15}$$

$$P = \begin{bmatrix} b & c_{\max} & c_{\min} & k & K \end{bmatrix} \tag{16}$$

$$s.t. \begin{cases} BA(P) < BA_{pass} \\ SWS(P) < SWS_{pass} \\ DTL(P) < 1.1 * DTL_{pass} \\ LB < P < UB \end{cases}$$

$$LB = [10,100,100,10,5000],$$

$$UB = [1000,10000,5000,1000,40000]. \tag{17}$$

where *BA(P)*, *SWS(P)*, and *DTL(P)* respectively indicate the RMS value of body acceleration, suspension working space and dynamic tire load of the optimized inertia suspension. BA_{pass}, SWS_{pass} and DTL_{pass} denote the RMS value of the corresponding performance indexes before optimization; *P* is the collection of the proposed suspension parameters to be optimized; *LB* and *UB* are the upper and lower bounds of their optimization, and the specific optimization process as shown in Fig. 6.

In this article, the RMS value of the vehicle body acceleration is the main optimization goal. However, the optimization effect is not ideal without deteriorating both the suspension working space and the dynamic tire load. But in the process of optimization, it is found that the constraint conditions, in equation (17), can be appropriately reduced to improve the optimization effect. Finally, after several simulation attempts, the constraint conditions of dynamic tire load (*DTL(P)*) are enlarged by 1.1 times. The optimized parameters of the proposed inertial suspension based on SH-PDD strategy are shown in Table 3.

TABLE 3. Relevant parameters of the proposed inertial suspension based on SH-PDD strategy.

Parameter	Value
Inertance b [kg]	196
Maximum damping coefficient $c_{\max}$ [N·s/m]	3044
Minimum damping coefficient $c_{\min}$ [N·s/m]	924
Suspension spring stiffness K [N/m]	10061
Suspension auxiliary spring stiffness k [N/m]	50

TABLE 4. Comparison table of RMS value of inertia suspension optimized by PSO.

	Before Optimization	After Optimization	Improvement
Body acceleration [m/s^2]	1.338	1.0986	17.9%
Suspension working space [m]	0.0112	0.0108	3.6%
Dynamic tire load [N]	806.51	877.13	-8.6%

The parameters in Table 3 are input into an inertial suspension model for simulation. The RMS values of vehicle body acceleration, suspension working space and dynamic tire load are obtained. As shown in Table 4, compared to the SH-PDD conventional suspension, the optimized SH-PDD inertial suspension significantly suppresses the body acceleration (improve 17.9%), makes full use of the advantages of an inertial suspension and improves the ride comfort. Therefore, the optimized SH-PDD inertial suspension is utilized as the reference model below.

V. DESIGN OF SLIDING MODE VARIABLE STRUCTURE CONTROLLER FOR INERTIAL SUSPENSION

The main goal of the design of the vehicle suspension system controller is to reduce the vehicle vibration caused by the bad road surface. This requires an accurate and fast controller to achieve these goals. In this article, variable-structure control system with sliding mode will be adopted to achieve these demand efficiencies, first proposed by former Soviet scholars [29]. Later, some scholars [30], [31] realized that the sliding mode variable structure control has invariability to the outside disturbance and perturbation, and further developed this control method [32]. The basic idea is to form a sliding mode in the error dynamics of the controlled suspension system and the ideal reference model. The proposed control scheme as shown in Fig. 7.

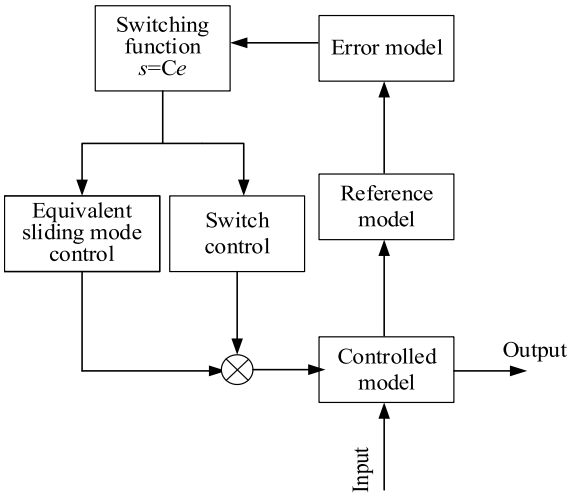

FIGURE 7. Flow chart of sliding mode variable structure control.

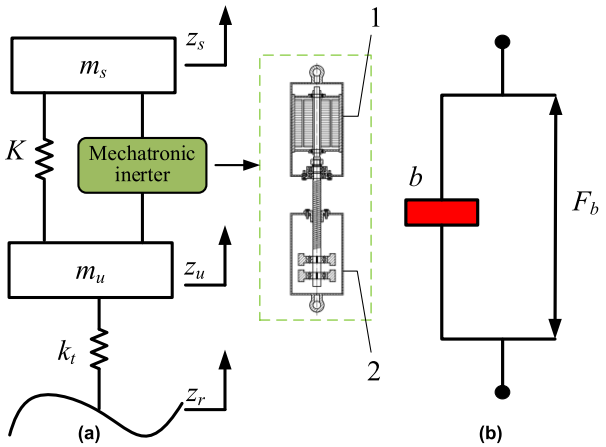

FIGURE 8. (a) the controlled model and (b) the equivalent model of the mechatronic inerter.

A. DESIGN OF SLIDING MODE VARIABLE STRUCTURE CONTROL SYSTEM

First, the optimized SH-PDD inertial suspension is utilized as the reference model, and the controllable inertial suspension model with mechatronic inerter is adopted as the controlled model [33]. The mechatronic inerter consists of a ball-screw inerter and a rotational electric machinery. It is equivalent to a controllable force (F_b) in parallel with an inerter (b), as pictured in Fig. 8. The controllable force is generated by adjusting the input current of the rotational electric machinery.

Where 1 and 2 denote the rotational electric machinery and the ball-screw inerter of a mechatronic inerter respectively.

The dynamic equation of the equivalent controlled model as given by:

$$\begin{cases} m_s\ddot{z}_s + K(z_s - z_u) \\ \quad +b(\ddot{z}_s - \ddot{z}_u) + F_b = 0 \\ m_u\ddot{z}_u + k_t(z_u - z_r) - K(z_s - z_u) \\ \quad -b(\ddot{z}_s - \ddot{z}_u) - F_b = 0 \end{cases} \tag{18}$$

where F_b denote the active output force of the mechatronic inerter, and b is the inertance.

According to the above dynamic model, the integration of the sprung mass displacement error, the spring mass displacement error and the spring mass velocity error of the controlled model and the reference model are defined as the tracking error vector (e):

$$e = [e_1, e_2, e_3]^{\mathrm{T}} = [\int (z_s - z_{sr}), z_s - z_{sr}, \dot{z}_s - \dot{z}_{sr}]^{\mathrm{T}} \tag{19}$$

Then the error dynamic equation can be written as, where $M = (m_s + b)\,(m_u + b)\text{-}b^2$.

The system switching surface function is defined as:

$$\begin{aligned} s &= Ce = [c_1, c_2, \cdots, c_n]\,[e_1, e_2, \cdots, e_n]^{\mathrm{T}} \\ &= c_1e_1 + c_2e_2 + \cdots + c_ne_n \end{aligned} \tag{21}$$

Generally, in this article, the value of c_n is 1, and according to the error vector, the value of n is 3.

Equation (21) is written as the following block matrix form:

$$\begin{aligned} \begin{bmatrix} \dot{e}_1 \\ \dot{e}_2 \end{bmatrix} &= \begin{bmatrix} 0 & 1 \\ 0 & 0 \end{bmatrix} \begin{bmatrix} e_1 \\ e_2 \end{bmatrix} + \begin{bmatrix} 0 \\ 1 \end{bmatrix} e_3 \\ &= \begin{bmatrix} 0 & 1 \\ 0 & 0 \end{bmatrix} \begin{bmatrix} e_1 \\ e_2 \end{bmatrix} + \begin{bmatrix} 0 \\ 1 \end{bmatrix} (s - c_1e_1 - c_2e_2) \\ &= \begin{bmatrix} 0 & 1 \\ -c_1 & -c_2 \end{bmatrix} + \begin{bmatrix} 0 \\ 1 \end{bmatrix} s \end{aligned} \tag{22}$$

When $\dot{s} = c_1e_2 + c_2e_3 + \dot{e}_3 = 0$, $s = c_1e_1 + c_2e_2 + e_3 = 0$.

$$\begin{aligned} \dot{e} &= A_e e + B_e U + H_e X_r \\ A_e &= \begin{bmatrix} 0 & 1 & 0 \\ 0 & 0 & 1 \\ 0 & -\dfrac{m_u K}{M} & 0 \end{bmatrix} \quad B_e = \begin{bmatrix} 0 & 0 & -\dfrac{m_u}{M} \end{bmatrix}^{\mathrm{T}} \\ H_e &= \begin{bmatrix} 0 & 0 & 0 & 0 & 0 \\ 0 & 0 & 0 & 0 & 0 \\ \dfrac{T(s) + c_s}{m_s} & -\dfrac{T(s) + c_s}{m_s} & \left(\dfrac{K}{m_s} - \dfrac{m_u K}{M}\right) & \left(\dfrac{m_u K - bk_t}{M} - \dfrac{K}{m_s}\right) & \dfrac{bk_t}{M} \end{bmatrix} \\ X_r &= \begin{bmatrix} \dot{z}_{sr} & \dot{z}_{ur} & z_{sr} & z_{ur} & z_r \end{bmatrix}^{\mathrm{T}} \end{aligned} \tag{20}$$

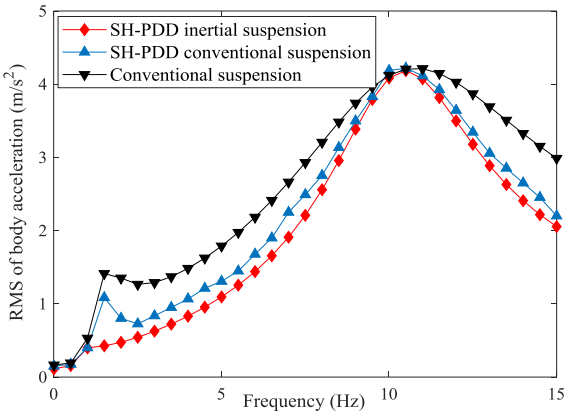

(a) RMS value of body acceleration

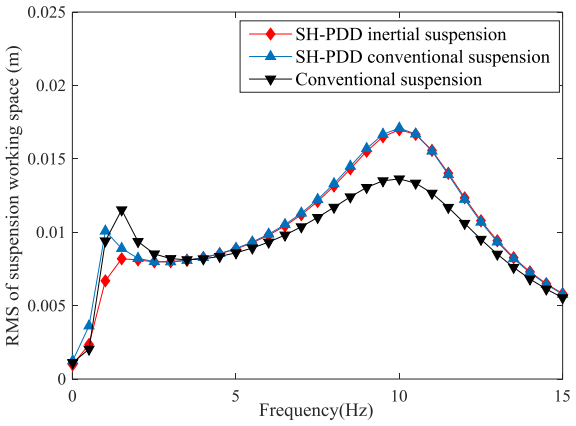

(b) RMS value of suspension working space

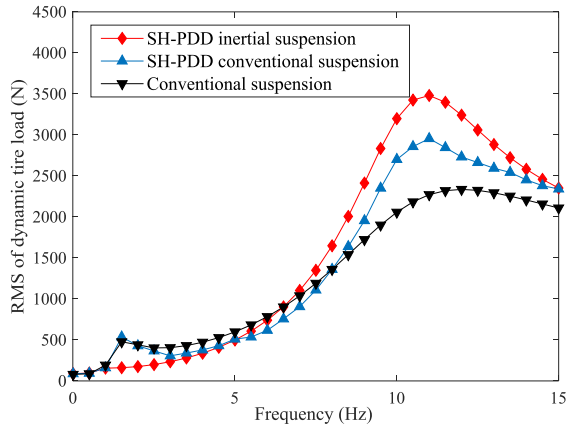

(c) RMS value of dynamic tire load

FIGURE 9. Performance comparison under the sinusoidal road.

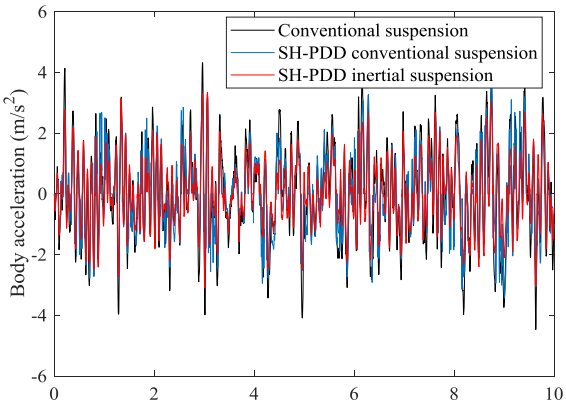

(a) Body acceleration

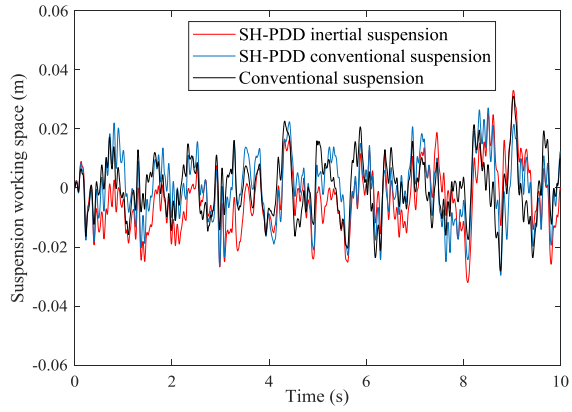

(b) Suspension working space

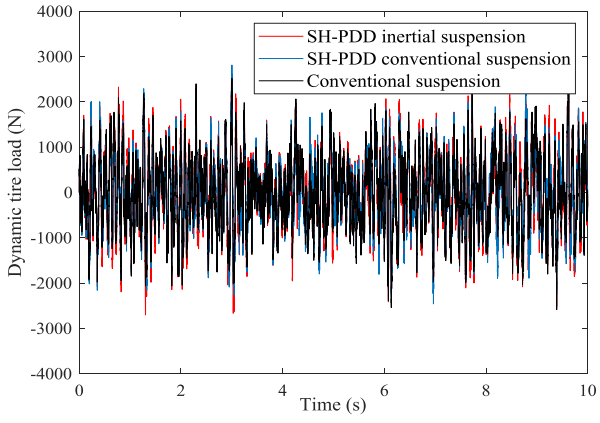

(c) dynamic tire load

FIGURE 10. Performance comparison under a random road condition with a vehicle speed of 20m/s.

Equation (22) can be simplified to:

$$\begin{bmatrix} \dot{e}_1 \\ \dot{e}_2 \end{bmatrix} = \begin{bmatrix} 0 & 1 \\ -c_1 & -c_2 \end{bmatrix} + \begin{bmatrix} e_1 \\ e_2 \end{bmatrix} \tag{23}$$

In this article, the pole assignment method is utilized to determine the desired closed-loop pole group. The characteristic polynomial of equation (20), as shown at the bottom of the previous page, is $D(\lambda) = \lambda_2 + c_2\lambda + c_1$, and the standard form of the transfer function of the second-order system is shown as:

$$\Phi(s) = \frac{w_n^2}{s^2 + 2\zeta w_n s + w_n^2} \tag{24}$$

Therefore, $c_1 = w_n^2$, $c_2 = 2\zeta w_n$.

Derivation of equation n (21) and make it equal to zero to obtain the following equation:

$$\frac{ds\,(x)}{dt} = C\dot{e} = C(A_e e + B_e U + H_e X_r) = 0 \tag{25}$$

The equivalent control force (F_b) in the sliding mode area can be obtained as:

$$F_b = -\left[CB_e\right]^{-1} C\,(A_e e + H_e X_r) \tag{26}$$

This article adopts the following law of constant velocity approach [34]:

$$\dot{s} = -\varepsilon sgns(\varepsilon > 0) \tag{27}$$

TABLE 5. Comparison of RMS values of performance index.

Suspension type	RMS of body acceleration /(m/s^2)	RMS of suspension working space /(m)	RMS of dynamic tire load /(N)
Conventional suspension	1.4855	0.0107	819.91
SH-PDD conventional suspension	1.2067	0.0108	840.67
SH-PDD inertial suspension	1.0064	0.0105	907.79

where ε denotes the approach speed of the system movement point to the switching surface $s = 0$.

According to the Lyapunov stability criterion: if $V(x)$ is positive definite and the derivation of $V(x)$ is negative definite, the system is asymptotically stable. The Lyapunov function selected in this article is:

$$V(x) = \frac{1}{2}s^{\mathrm{T}}s \tag{28}$$

Derivation of equation (28):

$$\dot{V}(x) = s^{\mathrm{T}}\dot{s} = s^{\mathrm{T}}(-\varepsilon \mathrm{sgn}(s)) \leq 0 \tag{29}$$

Therefore, the system is verified as stable.

Then the sliding mode control of the system is as follows:

$$u^* = F_b + [CB_e]^{-1}s = F_b - \frac{M}{m_u}\varepsilon \mathrm{sgn}(s) \tag{30}$$

The sliding mode control law of the system can be written as:

$$u = \begin{cases} u^*, & u^*(\dot{z}_s - \dot{z}_u) \geq 0 \\ 0, & u^*(\dot{z}_s - \dot{z}_u) < 0 \end{cases} \tag{31}$$

B. DYNAMIC PERFORMANCE ANALYSIS OF INERTIAL SUSPENSION SYSTEM

The sinusoidal road and the random road will be adopted in this article to verify the performance of an inertia suspension under sliding mode variable structure control. Firstly, the sinusoidal road with amplitude of 10 mm and frequency range of [0.1-15] Hz is utilized as input to simulate the RMS values of body acceleration, suspension working space and dynamic tire load. Simulation results are depicted in Fig. 9.

It can be illustrated from Fig. 9 that compared to the conventional suspension, the RMS value of body acceleration of the inertial suspension based on sliding mode variable

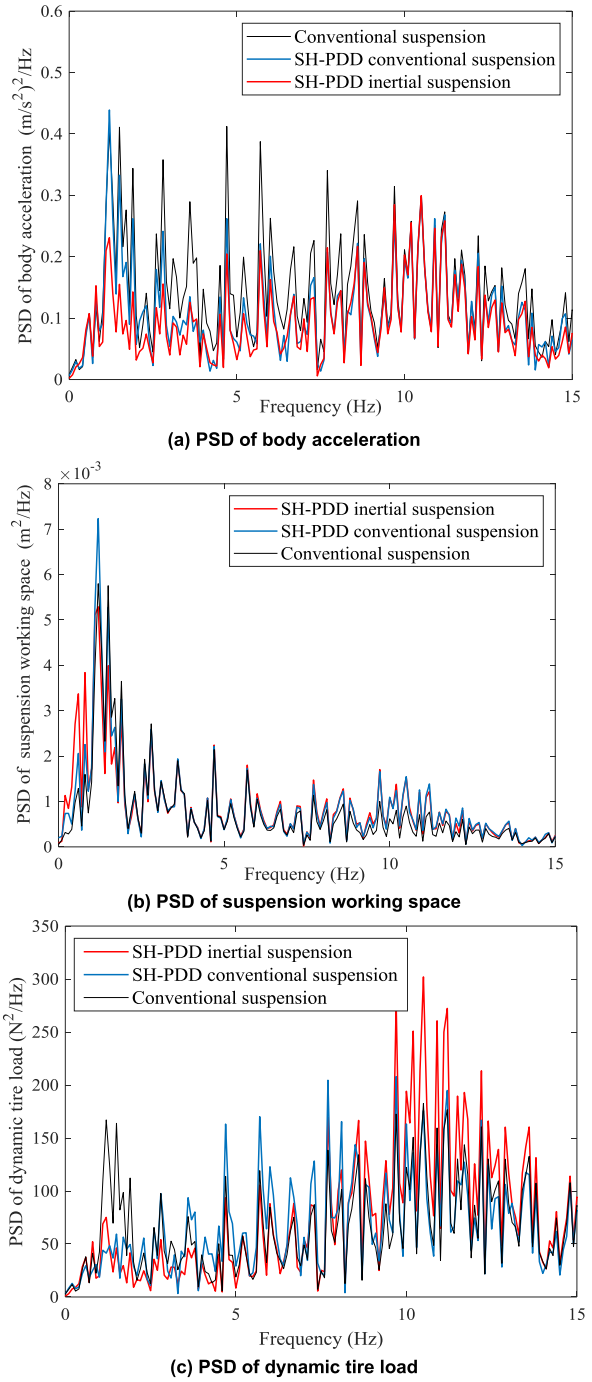

FIGURE 11. Comparison diagram of power spectral density.

structure control system is significantly reduced in the wide frequency domain, especially in a low frequency band, and the RMS value of suspension working space and dynamic tire load are also reduced in the low frequency band, but deteriorate at the high frequency resonance (near 10Hz). To sum up, under the sinusoidal road input condition, the proposed controllable inertial suspension perfectly realizes the vibration suppression performance in a wider range of body acceleration, and improves the ride comfort.

Under random road conditions with a vehicle speed of 20m/s, the simulation analysis of the performance

differences between an conventional suspension and an inertial suspension is shown in Fig. 10. The comparison of the performance RMS values is illustrated in Table 5.

It can be demonstrated from Fig. 10 and Table 4 that, under the conditions of a random road input, the RMS value of the body acceleration of an inertia suspension has been decreased significantly by 32.2%, compared with a traditional suspension. The RMS value of suspension working space also has been decreased by 1.9%. Therefore, an inertial suspension based on sliding mode variable structure control can effectively improve the vehicle comfort and achieve the expected control objectives. Fig. 11 shows the comparison of power spectrum density (PSD) of vehicle body acceleration, suspension working space and dynamic tire load under a random road condition.

As is shown in the Fig. 11, for the power spectral density of vehicle body acceleration, compared with the conventional suspension, the inertial suspension has a significant improvement in the frequency domain of the vehicle body, and also has different degrees of improvement in other frequency bands. However, for the power spectral density of the suspension working space and dynamic tire load, the proposed inertial suspension is better than the conventional suspension at a low frequency band, but it is not effective at high frequency. Overall, the proposed inertial suspension achieves the main purpose of improving the vehicle body acceleration and suppressing vibration in the wide frequency domain, especially in the low frequency range.

VI. CONCLUSION

This article has demonstrated successful application of SH-PDD control strategy in designing a semi-active vehicle inertial suspension system to suppress vibration in the wide frequency band for improve ride comfort. Firstly, an inertia suspension model and a traditional suspension model based on the SH-PDD control strategy are established and simulated. The simulation results show that compared with the conventional suspension, the proposed inertial suspension further reduces the peak value by 53.7% at the body resonance frequency. On the basis of the above good results presented, all parameters of the proposed inertia suspension are optimized by the PSO algorithm to further improve its performance. Then, the model of the optimized inertial suspension controlled by sliding mode variable-structure control system is designed and simulated. The simulation results show that compared with the SH-PDD conventional suspension and the conventional suspension, the RMS value of body acceleration of the SH-PDD inertial suspension is reduced by 16.6% and 32.2% respectively under a random road input condition, and the SH-PDD inertial suspension has a better suppression effect at low frequency, which is shown in the frequency domain. In general, on the basis of achieving vibration suppression in a wide frequency band, the proposed inertial suspension has a more prominent vibration suppression effect at low frequency than the traditional suspensions to improve ride comfort.

ACKNOWLEDGMENT

The authors would like to thank the associate editor and the anonymous reviewers for their careful reading and helpful comments.

REFERENCES

[1] D. Karnopp, M. J. Crosby, and R. A. Harwood, "Vibration control using semi-active force generators," *J. Eng. Ind.*, vol. 96, no. 2, pp. 619–626, May 1974.

[2] J. Yao, S. Taheri, and S. Tian, "A novel semi-active suspension design based on decoupling skyhook control," *Shock Vib.*, vol. 3, pp. 1318–1325, May 2014.

[3] C. Liu, L. Chen, X. Yang, X. Zhang, and Y. Yang, "General theory of skyhook control and its application to semi-active suspension control strategy design," *IEEE Access*, vol. 7, pp. 101552–101560, 2019.

[4] S. M. Savaresi, E. Silani, and S. Bittanti, "Acceleration-driven-damper (ADD): An optimal control algorithm for comfort-oriented semiactive suspensions," *J. Dyn. Syst., Meas., Control*, vol. 127, no. 2, pp. 218–229, Jun. 2005.

[5] S. M. Savaresi and C. Spelta, "Mixed sky-hook and ADD: Approaching the filtering limits of a semi-active suspension," *J. Dyn. Syst., Meas., Control*, vol. 129, no. 4, pp. 382–392, Jul. 2007.

[6] R. Morselli and R. Zanasi, "Control of port Hamiltonian systems by dissipative devices and its application to improve the semi-active suspension behavior," *Mechatronics*, vol. 18, no. 7, pp. 364–369, Sep. 2008.

[7] Y. Liu and L. Zuo, "Mixed skyhook and power-driven-damper: A new low-jerk semi-active suspension control based on power flow analysis," *J. Dyn. Syst., Meas., Control*, vol. 138, no. 8, May 2016, Art. no. 081001.

[8] P. Hang and X. Chen, "Integrated chassis control algorithm design for path tracking based on four-wheel steering and direct yaw-moment control," *Proc. Inst. Mech. Eng., I, J. Syst. Control Eng.*, vol. 233, no. 6, pp. 625–641, Jul. 2019.

[9] P. Hang, X. Chen, and F. Luo, "LPV/H_∞ controller design for path tracking of autonomous ground vehicles through four-wheel steering and direct yaw-moment control," *Int. J. Automot. Technol.*, vol. 20, no. 4, pp. 679–691, Aug. 2019.

[10] M. C. Smith, "Synthesis of mechanical networks: The inerter," *IEEE Trans. Autom. Control*, vol. 47, no. 10, pp. 1648–1662, Oct. 2002.

[11] R. Wang, X. Meng, D. Shi, X. Zhang, Y. Chen, and L. Chen, "Design and test of vehicle suspension system with inerters," *Proc. Inst. Mech. Eng., C, J. Mech. Eng. Sci.*, vol. 228, no. 15, pp. 2684–2689, Oct. 2014.

[12] X. Q. Sun, L. Chen, S. H. Wang, X. L. Zhang, and X. F. Yang, "Performance investigation of vehicle suspension system with nonlinear ball-screw inerter," *Int. J. Automot. Technol.*, vol. 17, no. 3, pp. 399–408, Jun. 2016.

[13] Y. Shen, L. Chen, and Y. Liu, "Influence of fluid inerter nonlinearities on vehicle suspension performance," *Adv. Mech. Eng.*, vol. 9, no. 11, Nov.2017, Art. no. 1687814017737257.

[14] M. C. Smith and F.-C. Wang, "Performance benefits in passive vehicle suspensions employing inerters," *Vehicle Syst. Dyn.*, vol. 42, no. 4, pp. 235–257, Dec. 2004.

[15] M. Z. Q. Chen, Y. Hu, C. Li, and G. Chen, "Performance benefits of using inerter in semiactive suspensions," *IEEE Trans. Control Syst. Technol.*, vol. 23, no. 4, pp. 1571–1577, Jul. 2015.

[16] Y. Shen, L. Chen, X. Yang, D. Shi, and J. Yang, "Improved design of dynamic vibration absorber by using the inerter and its application in vehicle suspension," *J. Sound Vib.*, vol. 361, pp. 148–158, Jan. 2016.

[17] L. Chen, C. Liu, W. Liu, J. Nie, Y. Shen, and G. Chen, "Network synthesis and parameter optimization for vehicle suspension with inerter," *Adv. Mech. Eng.*, vol. 9, no. 1, Jan. 2017, Art. no. 168781401668470.

[18] F.-C. Wang and H.-A. Chan, "Vehicle suspensions with a mechatronic network strut," *Vehicle Syst. Dyn.*, vol. 49, no. 5, pp. 811–830, Dec. 2010.

[19] Y. Shen, L. Chen, Y. Liu, X. Zhang, and X. Yang, "Improvement of the lateral stability of vehicle suspension incorporating inerter," *Sci. China Technol. Sci.*, vol. 61, no. 8, pp. 1244–1252, May 2018.

[20] Y. Shen, L. Chen, Y. Liu, and X. Zhang, "Modeling and optimization of vehicle suspension employing a nonlinear fluid inerter," *Shock Vib.*, vol. 15, Jul. 2016, Art. no. 2623017.

[21] Y. Hu, M. Z. Q. Chen, S. Xu, and Y. Liu, "Semiactive inerter and its application in adaptive tuned vibration absorbers," *IEEE Trans. Control Syst. Technol.*, vol. 25, no. 1, pp. 294–300, Jan. 2017.

[22] X.-J. Zhang, M. Ahmadian, and K.-H. Guo, "On the benefits of semi-active suspensions with inerters," *Shock Vibrat.*, vol. 19, no. 3, pp. 257–272, Dec. 2012.
[23] P. Li, J. Lam, and K. Cheung, "Investigation on semi-active control of vehicle suspension using adaptive inerter," in *Proc. 21st Int. Congr. Sound Vibrat. (ISCV)*, Beijing, China, Jul. 2014, pp. 3367–3374.
[24] X. Yang, L. Yan, Y. Shen, Y. Liu, and C. Liu, "Optimal design and dynamic control of an ISD vehicle suspension based on an ADD positive real network," *IEEE Access*, vol. 8, pp. 94294–94306, 2020.
[25] Y. Shen, Y. Liu, L. Chen, and X. Yang, "Optimal design and experimental research of vehicle suspension based on a hydraulic electric inerter," *Mechatronics*, vol. 61, pp. 12–19, Aug. 2019.
[26] M. Clerc and J. Kennedy, "The particle swarm–explosion, stability, and convergence in a multidimensional complex space," *IEEE Trans. Evol. Comput.*, vol. 6, no. 1, pp. 58–73, Feb. 2002.
[27] M. H. Ab Talib and I. Z. Mat Darus, "Intelligent fuzzy logic with firefly algorithm and particle swarm optimization for semi-active suspension system using magneto-rheological damper," *J. Vib. Control*, vol. 23, no. 3, pp. 501–514, Feb. 2017.
[28] A. J. Qazi, C. W. de Silva, A. Khan, and M. T. Khan, "Performance analysis of a semiactive suspension system with particle swarm optimization and fuzzy logic control," *Sci. World J.*, vol. 2014, pp. 1–12, Dec. 2014.
[29] V. I. Utkin, "Variable structure system with sliding mode," *IEEE Trans. Autom. Control*, vol. 22, no. 2, pp. 211–222, Dec. 1977.
[30] J. Yang, S. Li, and X. Yu, "Sliding-mode control for systems with mismatched uncertainties via a disturbance observer," *IEEE Trans. Ind. Electron.*, vol. 60, no. 1, pp. 160–169, Jan. 2013.
[31] H. Li, P. Shi, D. Yao, and L. Wu, "Observer-based adaptive sliding mode control for nonlinear Markovian jump systems," *Automatica*, vol. 64, pp. 133–142, Feb. 2016.
[32] R. Cui, L. Chen, C. Yang, and M. Chen, "Extended state observer-based integral sliding mode control for an underwater robot with unknown disturbances and uncertain nonlinearities," *IEEE Trans. Ind. Electron.*, vol. 64, no. 8, pp. 6785–6795, Aug. 2017.
[33] Y. Shen, J. Z. Jiang, S. A. Neild, and L. Chen, "Vehicle vibration suppression using an inerter-based mechatronic device," *Proc. Inst. Mech. Eng., D, J. Automobile Eng.*, vol. 234, nos. 10–11, pp. 2592–2601, Sep. 2020, doi: 10.1177/0954407020909245.
[34] C.-L. Hwang, "Sliding mode control using time-varying switching gain and boundary layer for electrohydraulic position and differential pressure control," *IEE Proc.—Control Theory Appl.*, vol. 143, no. 4, pp. 325–332, Jul. 1996.

XIAOFENG YANG received the B.S., M.S., and Ph.D. degrees in vehicle engineering from Jiangsu University, China. He is currently an Associate Professor with the School of Automotive and Traffic Engineering, Jiangsu University. His main research interest is the dynamic modeling and control of automotive engineering.

HANG SONG received the B.S. degree in automobile service engineering from Shandong Yingcai University. He is currently pursuing the M.S. degree with the School of Automotive and Traffic Engineering, Jiangsu University. His main research interest is the dynamic modeling and control of automotive engineering.

YUJIE SHEN received the B.S., M.S., and Ph.D. degrees in vehicle engineering from Jiangsu University, China. He is currently a Lecturer with the Research Institute of Automotive Engineering, Jiangsu University. His main research interests are dynamic modeling and control of automotive engineering and the design and modeling of new mechatronic inerter element.

YANLING LIU received the B.S. and M.S. degrees in vehicle engineering from Jiangsu University, China, where she is currently pursuing the Ph.D. degree with the School of Automotive and Traffic Engineering. Her main research interest is the dynamic modeling and control of automotive engineering.

TAO HE received the B.S. degree in automobile service engineering from Jiangsu University of Technology. He is currently pursuing the M.S. degree with the School of Automotive and Traffic Engineering, Jiangsu University, China. His main research interest is the dynamic modeling and control of automotive engineering.